# Imaging beamline for high energy proton radiography*

WEI Tao(魏涛)[1)] YANG Guo-Jun(杨国君) LONG Ji-Dong(龙继东)
WANG Shao-Heng(王少恒) HE Xiao-Zhong(何小中)

Institute of Fluid Physics, CAEP, P.O. Box 919-106, Mianyang 621900, China

**Abstract:** Proton radiography is a new tool for advanced hydrotesting. This article will discuss the basic concept of proton radiography first, especially the magnetic lens system. Then a scenario of 50 GeV imaging beamline will be described in every particular, including the matching section, Zumbro lens system and imaging system. The simulation result shows that the scenario of imaging beamline performs well, and the influence of secondary particles can be neglected.

**Key words:** proton radiography, beamline, image blur, MCS, collimator

**PACS:** 29.27.Eg **DOI:** 10.1088/1674-1137/36/8/019

## 1 Introduction

Classical radiography typically involves uncharged incident radiation such as X-rays and it allows one to see inside a complex structure without disturbing it. Till now, the flash X-rays radiography [1] is the experimental cornerstone of hydrodynamic research. In spite of numerous improvements in flash radiography over the past 60 years, the dose limitations, position resolution and backgrounds still limit the utility of such a technology [2]. Recently, a new idea, high energy proton radiography [3, 4], has provided a potential development direction.

In comparison with flash radiography, proton radiography has higher penetrating power, higher detection efficiency, less scattered background, inherent multi-pulse capability, more exact material identification and large standoff distance between test objects and detectors.

Proton radiography technique depends on the use of a particular magnetic lens to compensate for the small angle multiple Coulomb scattering (MCS) that occurs as the charged protons pass through the object. The use of such a magnetic lens turns the otherwise troubling complications of MCS into an asset. Protons undergo the combined processes of nuclear scattering, small angle Coulomb scattering, and energy loss, each with its own unique dependence on material properties. These effects make possible the simultaneous determination of both material amounts and material identification. This multi-phase interaction suite also provides the flexibility to tune the sensitivity of the technique to make it useful for a wide range of material thicknesses.

## 2 The magnetic lens system

When a proton beam passes through a dense object, the transmission rate, $N/N_0$, is given in terms of the path length $l$ through the object and the mean free path $\lambda$ by

$$N/N_0 = \mathrm{e}^{-l/\lambda}, \tag{1}$$

where $N_0$ and $N$ are the incident and surviving particle numbers respectively. The surviving protons undergo lots of MCS that produces a roughly Gaussian angular distribution [5] at the exit of the object, the half-width is

$$\varphi_0 = \frac{13.6\ \mathrm{MeV}}{\beta cp}\sqrt{\frac{L}{L_\mathrm{R}}}\left[1+0.038\ln\left(\frac{L}{L_\mathrm{R}}\right)\right], \tag{2}$$

where $p$ is the beam momentum in GeV/$c$, $\beta c$ is the beam velocity, $L$ is the path length through the object, and $L_\mathrm{R}$ is the radiation length of the material.

Received 11 November 2011

* Supported by Science and Technology Research Development Program of CAEP (2010A042016)

1) E-mail: weitaocaep@sohu.com

©2012 Chinese Physical Society and the Institute of High Energy Physics of the Chinese Academy of Sciences and the Institute of Modern Physics of the Chinese Academy of Sciences and IOP Publishing Ltd

High energy protons can be used to radiograph a dense object, however, a simultaneous angle divergency caused by MCS is unavoidable. A particular magnetic lens system [6] is used to focus the particles exiting from each point of the object onto a distant image plane. Without the lens, the MCS would seriously blur the radiography image. Furthermore, the magnetic lens system can provide angle sorting which allows the introduction of an angle cut aperture to aid material identification. Such a magnetic lens system was designed first by J. D. Zumbro at LANL, so it was also called the Zumbro lens.

The Zumbro lens system which consists of two identical FODO cells, as shown in Fig. 1, can achieve one-to-one imaging. In this case, the transfer matrix of one cell is

$$\vec{M}=\begin{bmatrix} M_{11} & M_{12} \\ M_{21} & M_{22} \end{bmatrix}=\begin{bmatrix} 1+\dfrac{L}{f}-\dfrac{LS}{f^2} & 2S+L-\dfrac{LS^2}{f^2} \\ -\dfrac{L}{f^2} & 1-\dfrac{L}{f}-\dfrac{LS}{f^2} \end{bmatrix}. \tag{3}$$

The above formula describes the single cell by thin-lens approximation, where $f$ is the focus length of the quadrupole magnet. The whole Zumbro lens can be expressed as

$$\vec{R}=\vec{M}\cdot\vec{M}=\mathrm{Tr}(\vec{M})\cdot\vec{M}-\det(\vec{M})\cdot\vec{I}. \tag{4}$$

where $\mathrm{Tr}(\vec{M})=M_{11}+M_{22}$ is the trace of $\vec{M}$, the determinant $\det(\vec{M})$=1. If the trace $\mathrm{Tr}(\vec{M})$=0, that is to say when

$$f^2=L\cdot S, \tag{5}$$

the whole transfer matrix $\vec{R}=-\vec{I}$ and the beamline can achieve one-to-one imaging.

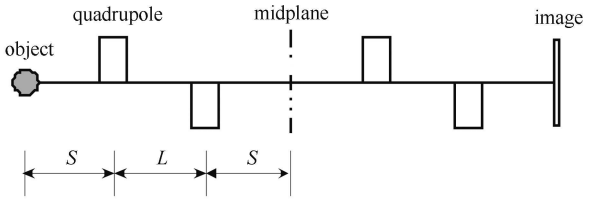


Fig. 1. The schematic of the Zumbro lens system.

The angle cut aperture must be placed where the rays are completely sorted by MCS angle; this always occurs in the midplane of a chromatically matched identity lens. Assuming a particle with initial coordinates $(x_0,\ \theta_0)$ passing through the object, neglecting the length of the object, the coordinates change to $(x_0,\ \theta_0+\varphi)$, and here $\varphi$ represents the angle deviation due to MCS. The position of this particle in the midplane is

$$x_{\mathrm{mid}}=M_{11}x_0+M_{12}\theta_0+M_{12}\varphi_0. \tag{6}$$

If we choose the initial beam strongly correlated,

$$\theta_0/x_0=\omega \quad \text{and} \quad \omega=-M_{11}/M_{12}, \tag{7}$$

in which $\omega$ is the correlation coefficient, the angle sorting function can be carried out.

Considering the particle's momentum deviation $\delta=\delta p/p$, the final position of this particle in the imaging plane is

$$\begin{aligned} x_{\mathrm{f}} &= (R_{11}+R'_{11}\delta)x_0+(R_{12}+R'_{12}\delta)(\theta_0+\varphi) \\ &= R_{11}x_0+R_{12}\theta_0+(R'_{11}+\omega R'_{12})x_0\delta+R'_{12}\varphi\delta. \end{aligned} \tag{8}$$

For the Zumbro lens, the second terms satisfy the equation [7] as follows,

$$R'_{11}+\omega R'_{12}=\mathrm{Tr}(\vec{M})'(M_{11}+\omega M_{12})=0. \tag{9}$$

Combining Eqs. (7–9), the final position is

$$x_{\mathrm{f}}=-x_0+R'_{12}\varphi\delta. \tag{10}$$

The remaining chromatic aberration blur depends on the deviation angle $\varphi$ and the momentum deviation $\delta$.

## 3 The 50 GeV beamline

Proton radiography requires a high energy beam to penetrate a thick object while keeping the MCS angle and energy loss small enough to allow good spatial resolution. Proton energy of 50 GeV is suitable to the design goal of 1 mm imaging blur. In this chapter,

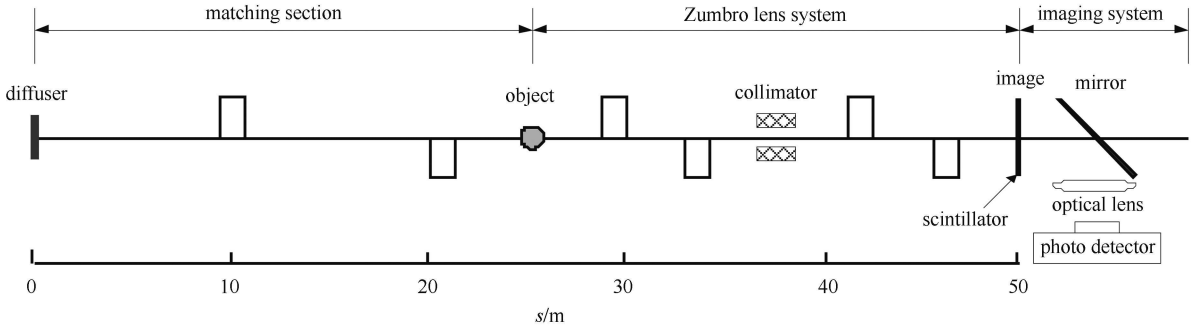


Fig. 2. The schematic of 50 GeV proton radiography beamline scenario.

we will introduce a scenario of 50 GeV proton radiography beamline, in which a matching section, the Zumbro lens system and imaging system will be particularized. Fig. 2 shows the schematic of 50 GeV proton radiography beamline scenario, and Fig. 3 shows the twiss parameters of the beamline.

### 3.1 The matching section

The required phase space correlations are provided by a matching section just upstream of the object. Moreover, this section must also expand the beam's transverse size to fully illuminate the field-of-view.

The matching section includes a diffuser and magnetic quadrupoles. The high energy proton beam passes through a thin diffuser, which gives a small angular divergence to the beam and then passes through a set of magnets, which introduces a correlation between the radial position of the proton in the object plane and its angle.

What is shown in Fig. 4 is the evolution diagram of a high energy proton beam in the matching section. The transverse emittance of the incident proton beam from the 50 GeV accelerator is about 0.2 πmm·mrad and the beam width is about 0.66 mm. The diffuser should adopt high $Z$ metal to decrease the transverse spread. An 18 mm tantalum plate is used to spread the 50 GeV beam, and the average scattering angle of the proton beam is about 2 mrad. Passing through the downstream 25.5 m matching section, the proton beam is enlarged long enough to illuminate the whole object.

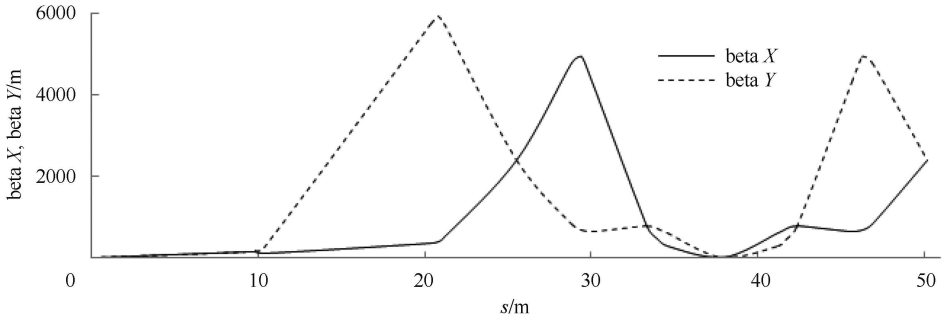


Fig. 3. The Twiss parameters of 50 GeV proton radiography beamline.

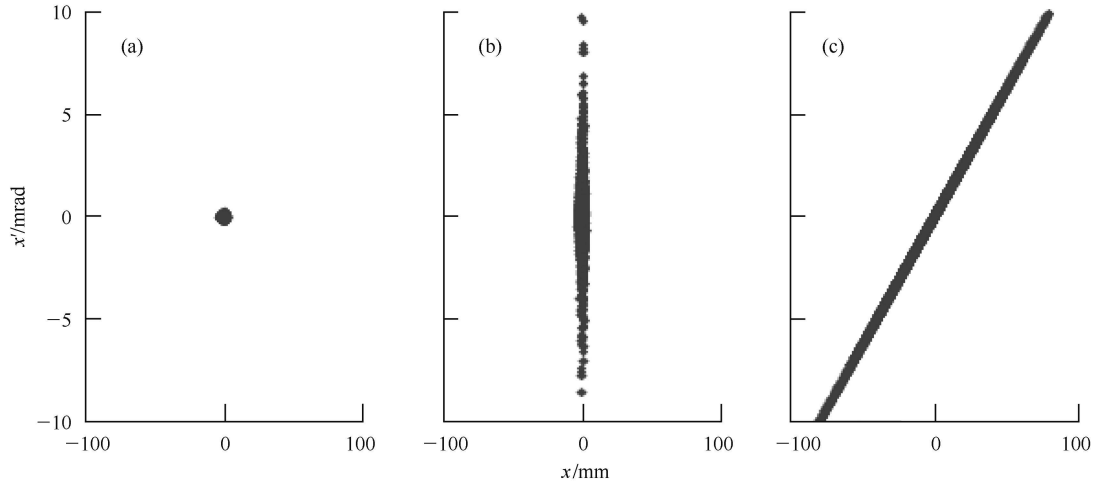


Fig. 4. Evolution diagram of transverse phase space. The horizontal phase space before the diffuser (a), after the diffuser (b), at the object plane (c).

### 3.2 The Zumbro lens system

To acquire perfect performance of the Zumbro lens for proton radiography, the chromatic aberration blur $R'_{12}\varphi\delta$ should be small enough. Both $\varphi$ and $\delta$ scale inversely with the beam momentum, so better resolution is expected with higher beam momentum. The chromatic coefficients [8] $R'_{12}$ (for $x$ direction) and $R'_{34}$ (for $y$ direction) are decided by the Zumbro lens system. In the case of thin-lens approximation,

$$R'_{12} = 4(L+S). \tag{11}$$

To decrease the chromatic coefficients, the feasible scheme is to increase the field gradients of the magnet lens. So the use of superconducting quadrupoles is suggested. Assuming the quadrupole's pole tip field of 5 Tesla, the lattice of the Zumbro lens system can be arranged within 24.6 m, and the chromatic coefficient is about 32 m.

In the center of the Zumbro lens system, the protons are sorted radially solely by their scattering angle in the object, regardless of which point in the object plane they originate from. This allows one to place a collimator at midplane and use it to make cuts on the MCS angle in the object. In the case of proton radiography, the collimator adopts a hole-type structure; the inner hole is empty and the proton beam can travel through, the outer layer is made of heavy metal which can prevent particles from passing through. With the collimator, one can limit the transmitted particles to only those with an MCS angle less than the cut angle. Furthermore, the collimator can shield a part of the secondary particles shower from the interaction between the proton beam and the object.

### 3.3 The imaging system

A light based detector system for proton radiography is shown in Fig. 2. Visible light is generated in a scintillator which is located in the image plane, reflected by a 45° mirror out of the path of the proton beam, and then collected and imaged by an optical lens onto the photon detector plane that creates the electrical signal. The photo detector is sensitive to charged particles and must therefore be out of the proton beam.

## 4 The simulation results

A great number of secondary particles are produced when a high energy proton beam impacts the object. The secondary particles shower includes gamma, neutron, proton, electron, π meson, etc. After being focused by a magnetic lens, the charged secondary particles are mostly lost before arriving at the imaging plane. Moreover, a majority of neutral particles are lost in the beam pipe. The ratio of the number of secondary particles which survive and the proton beam in the imaging plane is about 1:4. The distributions of survival of secondary particles are shown in Fig. 5, and 90% among them are gamma rays.

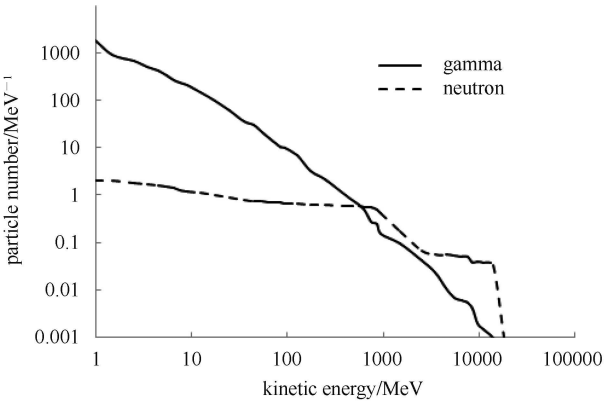


Fig. 5. The distribution of survival secondary particles in the imaging plane, the number of incident high energy protons is $1\times10^5$.

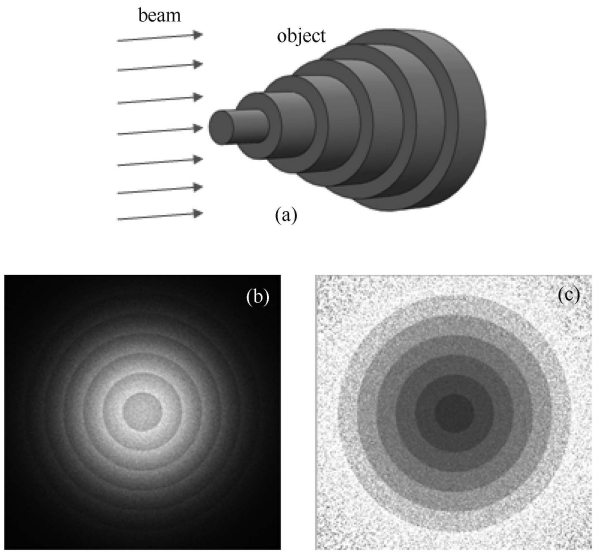


Fig. 6. Images from steel steps in simulation process. (a) Six-layered steel object, the thickness of each one is 30 mm; (b) Image with simulation data; (c) Image with simulation data divided by beam distribution.

Apart from the proton beam, the gamma rays also deposit energy in the scintillator and induce visible

light, although the photon flux is an order of magnitude lower than that of the proton beam. In fact, collimator can prevent a part of the gamma rays and reduce the influence by 60%–80%. The effect of secondary particles can be neglected.

Shown in Fig. 6 are the simulation results by Monte Carlo code GEANT4 [9]. The object is made up of six layers of steel plates, and the thickness of each one is 30 mm. The peak current of 50 GeV proton beam is 1.6 A and the beam pulse is 20 ns long; the transverse emittance is 0.2πmm·mrad. The simulation image is shown in Fig. 6(b); the number of macro particles is $2\times10^7$. Fig. 6(c) is the image getting rid of the influence of the proton beam distribution in the object, and one can identify the structure of the object more easily.

## 5 Conclusion

A high energy proton beam of 50 GeV can be used to radiograph a dense object. The simulation result shows the scenario of an imaging beamline should perform extremely well.

## References


1 DENG Jian-Jun, CHENG Lian-An, WANG Hua-Chen et al. Linear Induction Electron Accelerator. Beijing: National Defence Industry Press, 2006. 1–12 (in Chinese)
2 King N S P, Ables E, Ken Adams et al. NIMA, 1999, **424**(1): 84–91
3 Ziock H J, Adams K J, Alrick K R et al. The Proton Radiography Concept, LA-UR-98-1368. Available: http://lib-www.lanl.gov/la-pubs/00460235.pdf
4 Morris C L. Proton Radiography for an Advanced Hydrotest Facility, LA-UR-00-5716. Available: http://lib-www.lanl.gov/la-pubs/00357005.pdf
5 XIE Yi-Gang et al. Particle Detectors and Data Acquisition. Beijing: Science Press, 2003. 10–12 (in Chinese)
6 Thomas Mottershead C, Zumbro John D. Magnetic Optics for Proton Radiography. Proceeding of 1997 Particle Accelerator Conference, 1997, **2**: 1397–1399
7 SHI Jiang-Jun. High Energy Radiography Theory. Graduated Schoolbook for Chinese Academy of Engineering Physics, 2007. 271–273 (in Chinese)
8 HE Xiao-Zhong, YANG Guo-Jun, LIU Chen-Jun. High Power Laser and Particle Beams, 2008, **20**(2): 297–300 (in Chinese)
9 Agostinelli S et al. NIM A, 2003, **506**: 250–303. Available: http://geant4.web.cern.ch/geant4/